Available online at www.sciencedirect.com
SCIENCE DIRECT®
International Journal of Thermal Sciences 42 (2003) 571–581
International Journal of Thermal Sciences
www.elsevier.com/locate/ijts

The performance of a solar air heater with conical concentrator under forced convection

İnci Türk Toğrul *, Dursun Pehlivan

Fırat University, Faculty of Engineering, Chemical Engineering Department, 23279 Elazığ, Turkey

Received 8 February 2002; accepted 26 July 2002

Abstract

In this work, the efficiency of a new solar air heater with a conical concentrator, which can track the sun from sunrise to sunset, was investigated under forced convection conditions of air. The collector, whose absorber was arranged as a two-pass exchanger and mounted on the focal axis of the conical concentrator, was tested for a number of tilting angles and a variety of air mass flow rates.

In addition, major operation parameters related to efficiencies of the collector and heat flow in the absorber were determined and correlated with each other and compared with flat-plate solar collectors.

The highest efficiencies and maximum increase in the air temperatures were obtained at 28.4° tilting and the lowest mass flow rate, respectively. Although, the efficiencies were similar, the maximum outlet temperatures of the air were found to be approximately twice and heat transfer rates inside the absorber were higher than those reached by conventional flat-plate solar air heaters.

Keywords: Solar air heater; Conical concentrator; Two-pass collector; Heat transfer

1. Introduction

Solar collectors have a wide range of applications such as drying of agricultural products, space heating and air conditioning, industrial processes (textile, paper, etc.) and green house heating. Improving their performance is essential for commercial acceptance of their use in such applications. In the solar air heaters, energy in the form of radiation is transferred into air and even in the warmest climates, the flux of incident solar radiation is approximately up to 1100 $W \cdot m^{-2}$ without optical concentration. The solar air heaters occupy an important place among solar heating systems because of availability, minimal cost and the direct use of air as the working substance reduces the number of required system components. The primary disadvantage of solar air heaters is the need for handling relatively large volumes of air as a working fluid with low thermal capacity.

Many studies have been made on the enhancement of thermal performance of the solar collectors, using diverse materials of various shapes and different dimensions and layouts. The fact that the air has low thermophysical properties imposes the need to create a fully developed turbulent flow in order to increase the heat transferred between the absorber and the air stream. Thus, in the literature various collector designs have been postulated and tested for the objective of meeting this requirement. These include: the flat plate absorbers with the air flowing above, below or on both sides of the absorber [1–3]; V-folded absorbers in which the air flows parallel to the V-channels [4,5]; finned absorbers [6,7] and integrated collector/storage systems in which the heat storage tubes are transversely arranged inside the collector and air flows across these tubes [8] and flat and cylindrical metallic porous absorbers [9,10] and fabric polyester porous absorbers with plastic covers [11]. Jet plate solar collector [12] is another design in which multiple jets from the air stream below the absorber are mixed with the streams flowing above the absorber. Most of these collectors mentioned above have the dimensions of 5 to 10 m lengths, 0.6 to 1.3 m widths and 3 to 13 cm heights.

Concentrating collectors provide energy at temperatures higher than those of flat plate collectors. They concentrate and re-direct solar radiation into an absorber and usually require tracking of the sun. The collector types that have been recently proposed and studied can be broadly categorised as:

* Corresponding author.
E-mail addresses: incitogrul@yahoo.com (İ. Türk Toğrul), itogrul@firat.edu.tr (D. Pehlivan).

1290-0729/03/$ – see front matter
doi:10.1016/S1290-0729(03)00023-1

Nomenclature

A_a	view area of the concentrator	m^{-2}	
A_r	receiver area	m^{-2}	
C_p	specific heat capacity of the air	$W{\cdot}m^{-2}{\cdot}K^{-1}$	
D_H	hydraulic diameter	m	
F'	collector efficiency factor		
F_R	collector efficiency factor		
G	air flux	$kg{\cdot}hm^{-2}$	
h	film heat transfer coefficient	$W{\cdot}m^{-2}{\cdot}K^{-1}$	
I	direct solar radiation	$W{\cdot}m^{-2}$	
J_H	Colburn J factor		
k_f	thermal conductivity of the air	$W{\cdot}m^{-1}{\cdot}K^{-1}$	
L	the length of absorber tube	m	
m	mass flow rate of air	$kg{\cdot}s^{-1}$	
Re	Reynolds number		
Pr	Prandtl number		
St	Stanton number		
T_a	ambient temperature	°C	
T_f	local air temperature	°C	
T_i	inlet air temperature	°C	
T_o	outlet air temperature	°C	
T_p	absorber plate temperature	°C	
U_L	overall heat loss coefficient	$W{\cdot}m^{-2}{\cdot}K^{-1}$	
ΔT	air temperature rise, $= T_o - T_i$	°C	
q_u	heat flux	$W{\cdot}m^{-2}$	
Q_u	heat transfer rate	W	

Greek symbols

α	absorbtivity of the absorber
γ	fraction of the radiation reflected on the absorbing surface of the receiver
η	collector efficiency
μ_f	viscosity of air ..... $kg{\cdot}ms^{-1}$
θ	slope angle of collector
ρ	reflectivity of the concentrator
ρ_f	density of air ..... $kg{\cdot}m^{-3}$
τ	transparent cover transmittance
$(\tau\alpha)_e$	the effective transmittance absorbance product

(i) reflective and (ii) refractive units. These types focus on a line in cylindrical concentrators or on a point in circular ones. Concentrating solar collectors of different geometric shapes, sizes and orientation are in use today. Many of these have quite novel and unique appeal. Much of the novelty are related with the means making the collectors more efficient in collection of solar radiation.

Conical parabolic collectors have a very high concentration ratio. Smith [13] patented a collector with a conical surface, which directed convergently reflecting rays at an absorber positioned in the central focal axis. Uroshevich [14] patented a focusing-type solar collector system which consists of a parabolic tough with an interior reflective surface that faces the main reflector of the collector. McLean [15] describes a system using fibre optics in a fixed ray to maximise the variations of the sun inclination as it travels through the sky.

Evacuated tubes are used to reduce heat losses from the receiver. Some of the earlier patents are those of Mather and Sherlock [16], in which the tube was placed in a transparent Pyrex glass jacket. Sims [17] invented a solar energy receiver which could also be used as a high concentration ratio compound parabolic collector. O'Neill [18] has a patent on a curved prismatic Frensel-type lens. Winston [19] invented a solar collector with a refractive element and an ideally contoured wall with a reflective surface.

Although, the collectors of focusing type are used extensively in liquid heating, there is not much work on their usage in air heating. Also, any conical focusing system tracking the sun have not been met among the collectors mentioned above. So, it can be considered that studies on such collectors are necessary to gain additional data on the utilisation of solar energy.

In this study, therefore, a solar collector with conical concentrator having a cylindrical absorber for heating air is designed, constructed and tested in the forced convection conditions. The primary consideration in designing such a collector is to attain high collector efficiencies and thus to obtain air flows at higher temperatures than those from conventional flat-plate collectors. For this respect, the collector differs from most collectors described in the literature.

2. Analysis

The commonly accepted method for measuring the steady state efficiency of solar collectors depends on the following equation [20].

$$\eta = F_R(\tau\alpha)_e - F_R U_L(T_i - T_a)/I \tag{1}$$

In this equation three parameters (F_R, $(\tau\alpha)_e$ and U_L) describe the performance of the collector. These parameters are directly associated with the design of the collector, flow conditions and construction materials.

Hottel and Whillier gave [21] an equation, which enables one to compute the heat removal factor. Following this work, Bliss [22] derived several efficiency factors (F' values) for different types of collectors. These equations given below with the description of efficiency factors apply to water type collectors and to one special case of air type collectors.

$$F_R = (GC_p/U_L)\left[1 - \exp(-F'U_L/GC_p)\right] \tag{2}$$

F' = (actual useful heat collectionrate) × (useful heat collection rate obtainablewith entire collector surface at average fluid temperature)$^{-1}$

F_R = (actual useful heat collectionrate) × (useful heat collection rate obtainablewith entire collector surface at fluid entering temperature)$^{-1}$

Eq. (1) is known as the Hottel–Whillier–Bliss equation or the generalized performance equation. The usefulness of its development is evident by considering the following three steady-state thermal performance expressions.

$$q_u = (\tau\alpha)_e I - U_L(T_p - T_a) \tag{3}$$

$$q_u = F'\big[(\tau\alpha)_e I - U_L(T_f - T_a)\big] \tag{4}$$

$$q_u = F_R\big[(\tau\alpha)_e I - U_L(T_i - T_a)\big] \tag{5}$$

The prediction of thermal performance of a collector, requires firstly determination of collector parameters for $(\tau\alpha)_e$, U_L and insertion of ambient values for I and T_a, then the difficult task of estimating absorber plate temperature T_p by Eq. (3). Average fluid or fluid inlet temperatures are used in Eqs. (4) and (5), respectively. They are often known or can be more accurately estimated or specified. Similar efficiency expressions may be written for concentrating collectors as shown below:

The useful energy per collector aperture, Q_U/A_a, of a concentrating air collector operating under assumed steady-state conditions is given below [23].

$$\frac{Q_U}{A_a} = F_R I(\gamma\tau\alpha)_e\rho - F_R U_L \frac{A_r}{A_a}(T_i - T_a) \tag{6}$$

The term, $(\gamma\tau\alpha)_e\rho$, represents the optical properties of the system. The intercept factor, γ, is defined as the reflected fraction of the incident radiation on the absorbing surface of the receiver. τ is the transmittivity of transparent cover. α and ρ are the absorptivity and the reflectivity of the absorber and concentrator, respectively.

Overall collector efficiency, η, is then given by the following equation:

$$\eta = \frac{Q_U}{A_a I} = F_R(\gamma\tau\alpha)_e\rho - F_R U_L \frac{A_r}{A_a}\left(\frac{T_i - T_a}{I}\right) \tag{7}$$

The following equation can also be used to estimate the collector efficiency values.

$$\eta = (mC_p/A_a I)(T_o - T_i) \tag{8}$$

Eq. (7) indicates that a plot of efficiency against $(T_i - T_a)/I$ will result in a straight line whose slope and intercept are $F_R U_L A_r/A_a$ and $F_R(\gamma\tau\alpha)_e\rho$, respectively. Thus, if the optical properties of the system are known, F_R and U_L can be determined.

The general methodology [24,25] was approved and used to find heat transfer rates and coefficients in the absorber. The forced convection heat transfer coefficient for a smooth absorber can be obtained from the Blasius and Dittus–Boelter equation.

$$h = 0.023\frac{k_f}{D_H} Re_H^{0.8} Pr^{0.6} \tag{9}$$

Table 1
Error sources in the system

Parameters	Error
Errors in temperature measurements:	
Thermocouple errors	±0.25–0.5 °C
Errors due to fitting elements	±0.1 °C
Measurement errors	±0.25 °C
Total potential error in recording each temperature = ±0.367–0.567 °C	
Mean error in determining times of periodical temperature measurements = ±0.1 min	
Errors in flow rate measurements	
Error due to anemometer	±0.1 m·s^{-2}
Error due to leakage	±0.1 m·s^{-1}
Total potential error in flow rate measurements = ±0.1414 m·s^{-1}	
Error in solar energy measurements:	
Error due to piranometer	±0.01 W·m^{-2}
Errors due to fitting elements	±0.1 W·m^{-2}
Total potential error in solar energy measurements = ±0.1 W·m^{-2}	
Total potential error due to sun tracking system = ±0.5°	
Other errors = ±0.1–0.2%	

where, $Re_H = GD_H/\mu_f$ and $Pr = \mu_f C_p/k_f$.

Average values of the heat transfer coefficient so determined have been used to evaluate the Stanton number and J_H factor:

$$St = \frac{h}{GC_p} \tag{10}$$

$$J_H = St(Pr)^{2/3} \tag{11}$$

Because the accuracy of the temperature measurements are main error sources (Table 1) in the results, error estimation depend mostly on mean reading errors of the thermocouples at six points and the numerical accuracy of the other parameters. Considering the relative errors in the individual factors denoted by x_n, error estimation was made using the following equation and they have changed ±% 1.05–1.50.

$$W = \big[(x_1)^2 + (x_2)^2 + \cdots + (x_n)^2\big]^{1/2} \tag{12}$$

3. Heater details and instrumentation

The experimental set-up and the important size parameters of collector are shown in Fig. 1 and in Table 2, respectively.

The conical solar collector was constructed from 0.5 mm thickness stainless steel sheets and mounted on the main iron pipe outer surface of which painted with black collector paint. This assembly was placed on a four-wheeled table by means of two arms, which could also serve to set the collector tilting.

The copper absorber tube placed on the focal axis of the concentrator was arranged as a two-pass exchanger. Outer surface of this tube is also painted with black collector paint and cupped with a transparent glass tube.

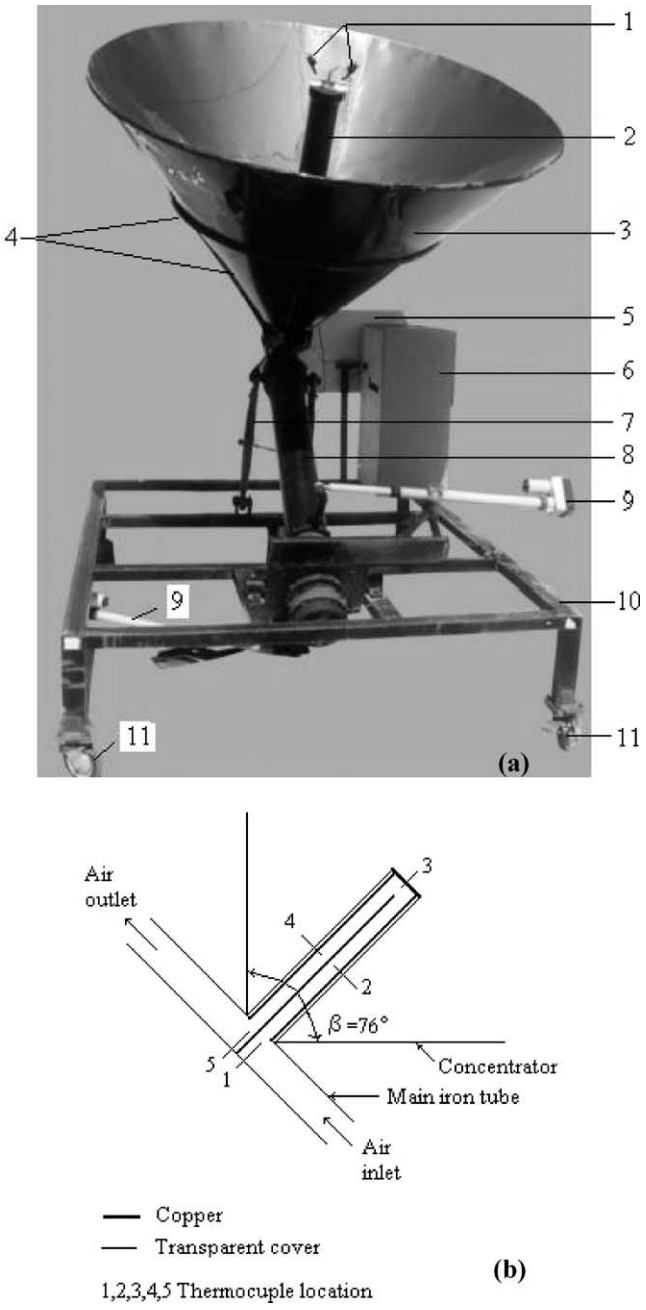

Fig. 1. (a) Solar air heater with conical concentrator. (1, photocells; 2, absorber; 3, conical concentrator; 4, conical concentrator supporting frame; 5, tracking unit; 6, temperature measurement unit; 7, the arms for setting tilting; 8, main air flow tube; 9, moving arm and driving system for tracking; 10, collector table; 11, wheels); (b) the schematic view of absorber tube.

The system is able to rotate via two satellite antenna motors to face conical concentrator continuously towards the sun. The motors driven by two photocells located on the head of the absorber sustained the movement and maintained tracking from sunrise to sunset. All the details of the solar air heater are given elsewhere [27].

The air heater was oriented to south and tilted to form angles of 28.4, 33.4 or 38.4° between main tube and horizontal surface (local latitude 38.4°). The incident solar radiation was measured with a Kipp–Zonen solarimeter connected to a recorder.

Table 2
The characteristics of conical solar collector

A_r	0.295 m^2
A_a	2.22 m^2
β (koni iç açısı)	76°
Collector tilt, θ	28°.4′, 33°.4′, 38°.4′
Absorber	Copper
Absorber inner diameter	10.0 cm
Absorber outer diameter	10.2 cm
Transparent cover	Bore silicate glass ($n_d = 1.473$, $\tau = 0.9183$, $\rho_d = 0.0697$, $\alpha = 0.012$)
Cover inner diameter	11.4 cm
Cover outer diameter	12.0 cm
Black collector paint	$\alpha = 0.98$, $\varepsilon = 0.88$
$(\gamma\tau\alpha)_e$ for black collector paint	0.9012
Concentrator	18–10 Cr–Ni stainless steel
γ	1 [26]

The air was supplied by a small blower at the inlet port of the main iron pipe and it's flow rate was measured with an anemometer at the exit as well as wind speeds. Air temperatures at the inlet, outlet and 0.46 m equally distanced five points in the space along the length of the absorber and ambient temperatures were measured at 30 minutes intervals by Fe-constantan thermocouples connected to a multi channel-temperature measurement unit.

4. Results and discussion

4.1. Collector efficiency

The experiments on the performance of solar air heater were carried out from July to September in 1999 (Elazığ/Turkey, local latitude is 38.4°).

Typical hourly values of global and direct solar radiation recorded with pyranometer and ambient temperatures between 7 a.m. and 5 p.m. are shown in Fig. 2. The figure indicates that the direct and global solar radiations are at their highest values at noon (at about 12.30 p.m.) as expected. The diffuse radiation slightly decreases as the time passes afternoon.

The performance tests have been carried out according to the international standard methods [23,28]. In the experiments, the mass flow rate of air and the tilting angle of the solar air heater are varied from 30 to 70 kg·hr^{-1} and from 28.4 to 38.4°, respectively.

The different curves given in Fig. 3 show the variation in the daily mean temperatures of the air stream at a number of points along the length of the main tube. The horizontal axis values in this figure show the distances from the tube inlet. Then, 0.92 m distance coincide U-section of the absorber tube and 1.84 m tube outlet accordingly. The temperature of the air in the absorber tube is seen to decrease steadily with its mass flow rate and increase along the tube length for all

Table 3
Operating conditions and rises in the air temperatures (ΔT) in some studies on flat-plate solar collectors

Operating conditions	Ti (°C)	ΔT (°C)	η	Reference
collector length = 3.66 m	20	31.66	–	[29]
$Re = 10^4$	40	16.11	–	
collector length = 9.10 m,				[30]
$I = 800$ W·m^{-2}, $m = 504$ kg·hr^{-1}	–	23.4	0.3991	
$m = 862$ kg·hr^{-1}	–	17.4	0.5029	
$I = 950$ W·m^{-2}, collector length = 5 m,				[31]
$G = 0.027$ kg·sm^{-2}				
Flow above and below	24	13	–	
V-folded absorber	25	8	–	
Corrugated duct absorber	25	15	–	
$G = 0.011$ kg·sm^{-2}				
Flow above and below	24	19	–	
V-folded absorber	25	15	–	
Corrugated duct absorber	25	29	–	
The length of absorber = 1.56 m at solar noon				[32]
Single pass	–	17.2	0.58	
Double pass	–	23.88	0.68	
Single channel design with single air flow between absorber and bottom plates with no isolation				[1]
$m = 93.6$ kg·hr^{-1}, $V = 0.63$ m·s^{-1}, $I = 900$ W·m^{-2}, $Re = 3300$, $L = 6.75$ m,	33.5	16.1	–	
Same, with bottom isolation provided: $m = 97.2$ kg·hr^{-1}, $V = 0.62$ m·s^{-1}, $I = 900$ W·m^{-2}, $Re = 3400$, $L = 9$ m,	33.7	25.2	–	
Double channel design with single air flow between absorber and bottom plates and bottom isolation provided $m = 93.6$ kg·hr^{-1}, $V = 0.48$ m·s^{-1}, $I = 900$ W·m^2, $Re = 3300$, $L = 9$ m	53.7	34.1	–	
Double channel design with double air flows between top glass and absorber plate and between absorber and bottom plates and with bottom isolation provided $m = 46.44$ kg·hr^{-1}, $V = 0.50$ m·s^{-1}, $I = 694$ W·m^{-2}, $Re = 4900$, $L = 5.9$ m	33.2	25.7	–	

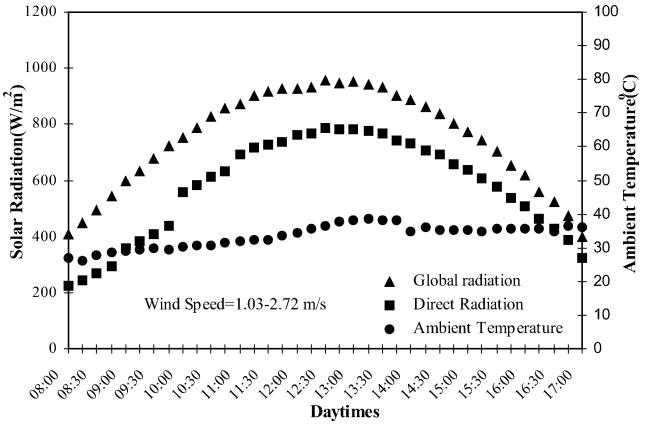

Fig. 2. Hourly variation of solar radiation and ambient temperature.

the tilting angles. The decrease in the temperatures of air at high rates is not so much as expected, implying somewhat enhancement in heat transfer because of increasing turbulence. As shown here, air temperatures decrease with the angle of tilting, the highest values are obtained at the lowest 28.4° angle of tilt and it is lowest at the local latitude value. This may be attributed to one-dimensional tracking the sun that enables conical concentrator to receive solar radiation normal to the view surface longer times before and after the noon. The conical collector set at local latitude angle can receive solar radiation vertically and complete reflection to the absorber occurs only on the summer days between 9–10 a.m. and 14–15 p.m. As the incident solar radiation in these periods is less intensive than that at noon, the air passing through the absorber is heated lesser compared to the other setting angles. The maximum air outlet temperatures at this tilting vary from 68 °C to 82 °C depending on the mass flow rate of air as shown in Fig. 4. These temperatures are approximately twice those reached by conventional flat-plate solar collectors with empty air space. Some collectors acquiring similar temperature differences and efficiencies are seen to have absorber lengths at least twice that of the present collector (1.84 m) as are given in Table 3 [29–32].

The changes in the air temperature rise ($T_o - T_i$) against direct radiation and airflow rate are shown in Figs. 5 and 6, respectively. Each line in Fig. 5 was drawn by using regression equation, which fits best the changes in all the daily temperature and direct radiation values. The temperature rise, ΔT, increases linearly with the incident direct radiation reaching the maximum value at noon (800 W·m^{-2}) on the surface of the conical collector, and decreases with the increasing air flux. The maximum temperature rise is ob-

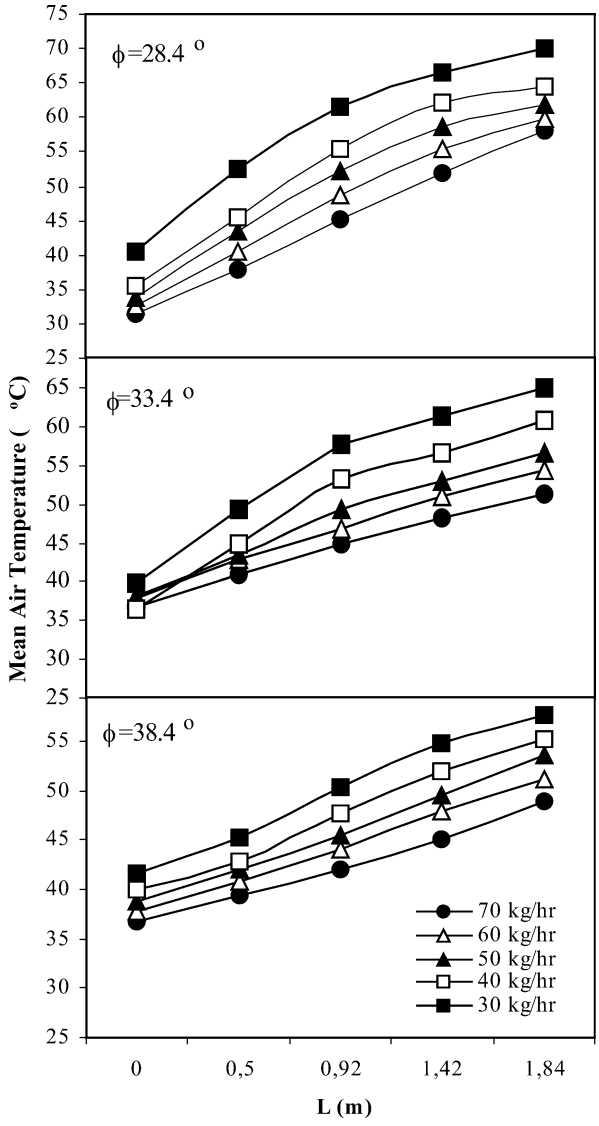

Fig. 3. The changes in the air temperatures inside the absorber tube.

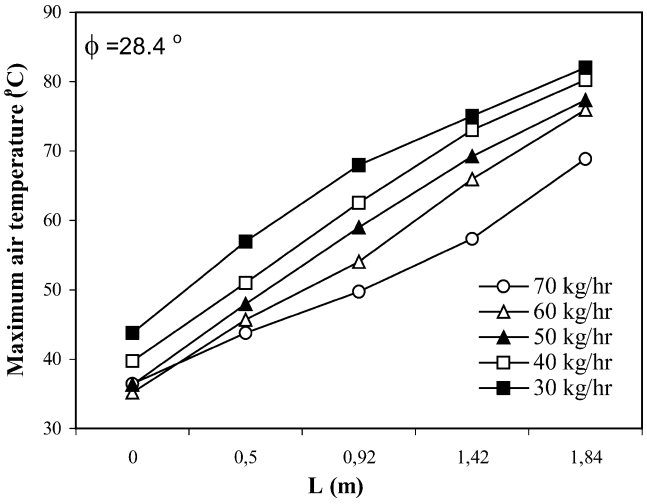

Fig. 4. The changes in the maximum air temperatures inside the absorber tube at solar noon for 28.4° tilting of the solar collector.

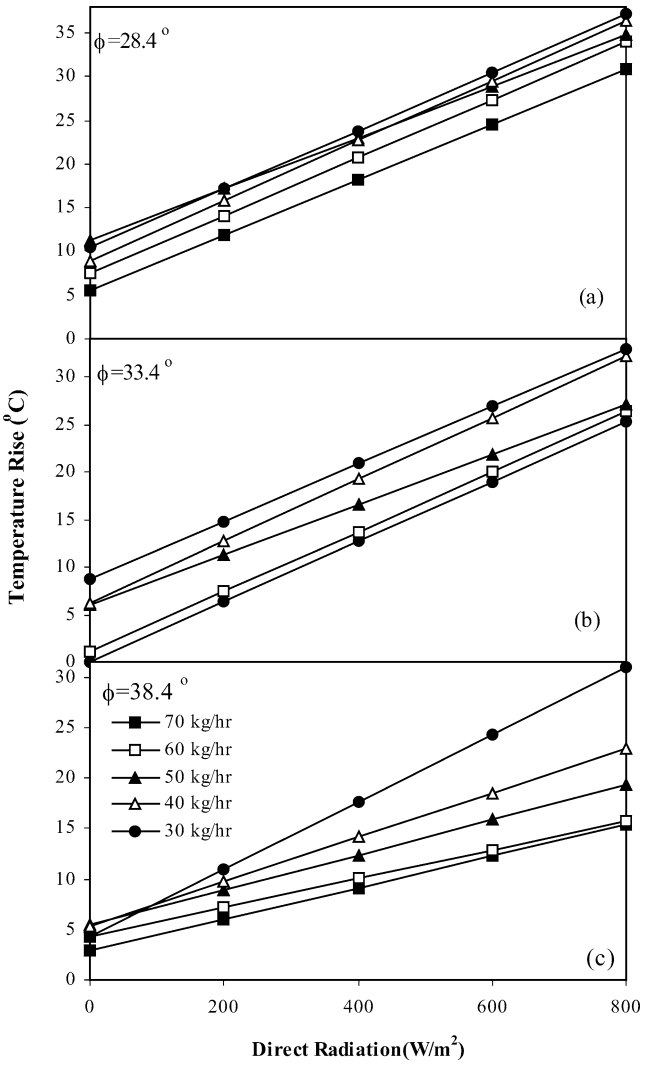

Fig. 5. The variation of ΔT with the incident solar radiation for various tilting angles and air flow rates.

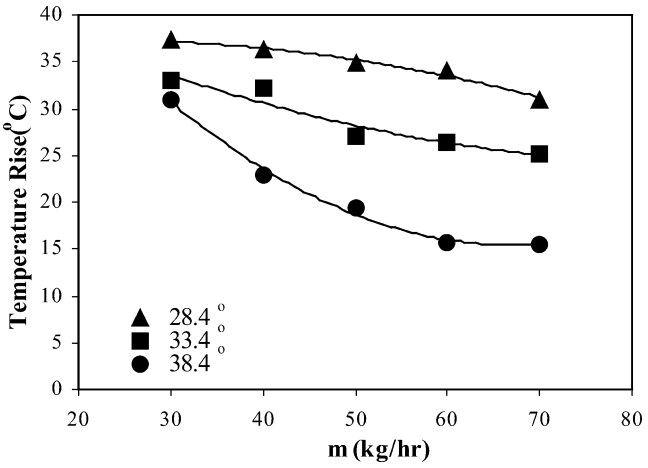

Fig. 6. The variation of the increase in the air temperatures recorded at solar noon with the mass flow rates of the air for various tilting angles.

Table 4
The increases ΔT (°C) in the air temperatures at noon

Air flow rate (kg·hr^{-1})	Tilting angle		
	28°.4′	33°.4′	38°.4′
70	30.9	25.3	15.5
60	34.1	26.3	15.8
50	34.8	27.1	19.3
40	36.4	32.1	22.9
30	37.2	32.9	30.9

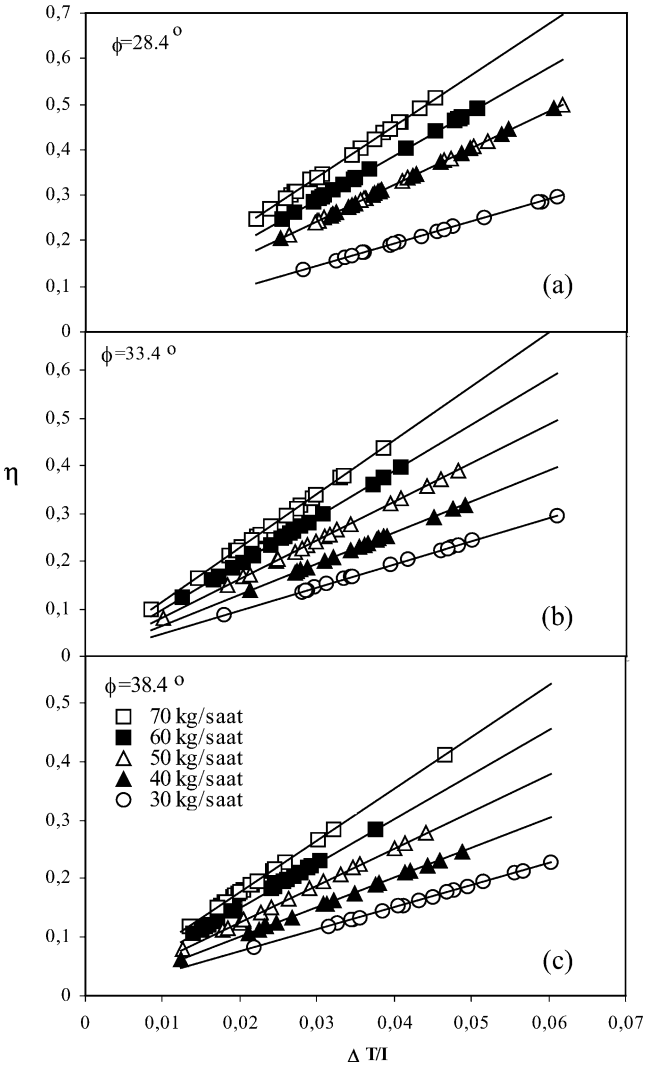

Fig. 7. The changes in efficiencies with $\Delta T/I$ for various air flow rates and the tilting angles.

tained at 28.4° tilting angle and at the lowest 30 kg·hr^{-1} air flow rate. These results are expected, because more solar radiation fell vertically on the conical collector and more heat accumulation occurs in the absorber during the summer days at the tilting angle 10° lower than the local latitude. In addition, outlet temperatures of the air increases due to it's prolonged contacting times at lower flow rates inside the absorbing tube. The increases in the air temperatures at noon are compared quantitatively in Table 4.

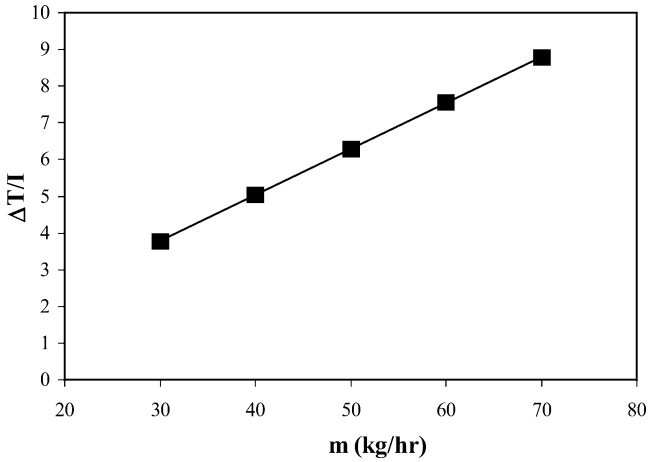

Fig. 8. The changes in $\Delta T/I$ with air flow rates.

Fig. 7 shows variation of the collector efficiencies, η, against $\Delta T/I$ values for various tilting angles and air flow rates. It is seen here that the useful energy $Q_u = \dot{m}C_p\Delta T$ and the collector efficiency η increase continuously with the airflow rate. In the same way, the data plotted in Fig. 8, which depicts the variation in the $\Delta T/I$ values as a function of mass flow rate of air, supports these results.

Fig. 9 shows the typical efficiency curves plotted using Eq. (7) at different tilting angles and air flow rates. The conversion efficiency of incident solar radiation into heat energy in the collector were computed by using data from the daytime measurements between 11.00 a.m. and 2 p.m. at the symmetrical times to the solar noon. Because they are the values from the measurements before and after the noon, the data points show a scattered pattern under and over the regression line.

It is clearly seen here that, although the measured data points are mostly scattered, they can still be used to evaluate $F_R(\gamma\tau\alpha)_e\rho$ and $F_R U_L A_r/A_a$ coefficients in Eq. (7). from the least squares fit of linear regression. A quantitative comparison of the calculated thermal performance and F_R values of the present solar collector is tabulated in Table 5 and the effect of air flow rate on the efficiencies is shown in Fig. 10. These values increase as the mass flow rate of air increase. This may be attributed to the decreased thermal losses to the ambient. The values of $F_R(\gamma\tau\alpha)_e\rho$ for 70 kg·hr^{-1} are much higher than those for the other air flow rates. The efficiencies and F_R values considerably increase as tilting angles decrease. This is due to better view of sun at low angles. Although, instantaneous efficiencies increase with both flow rate and temperature rise of the air as implemented by Eq. (8), the rise in the air temperature decrease with air flow rate especially at the highest tilting angle where solar radiation does not fell vertically on the conical concentrator even at noon. For this reason, the effect of air flow rate on the instantaneous efficiencies is more pronounced. The speed of the wind in the ambient air has also some influence on the air temperature rise.

Table 5
Performance and F_R values of the conical collector for various mass flow rate of air

Air flow rate (kg·hr^{-1})	Tilting angle					
	η			F_R		
	28°.4′	33°.4′	38°.4′	28°.4′	33°.4′	38°.4′
70	0.5030	0.4990	0.2898	0.886	0.879	0.514
60	0.4071	0.4242	0.1963	0.717	0.747	0.346
50	0.3688	0.3315	0.1813	0.650	0.584	0.319
40	0.3492	0.3025	0.1785	0.620	0.533	0.314
30	0.2935	0.2531	0.1777	0.517	0.446	0.313

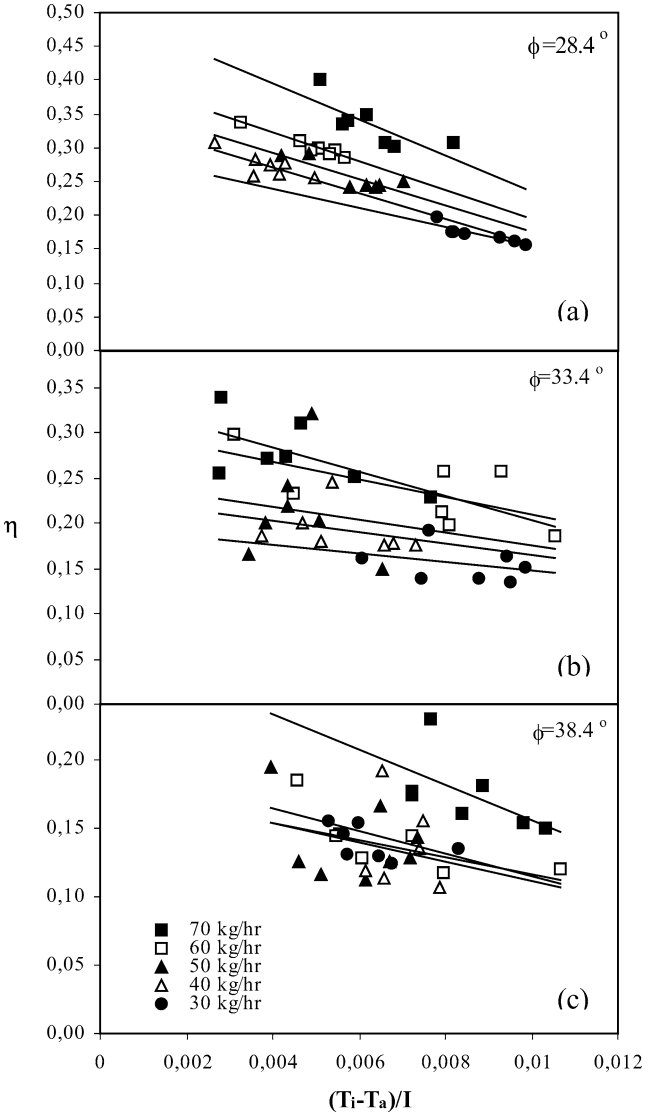

Fig. 9. The changes in instantaneous efficiencies for various air flow rates and the tilting angles.

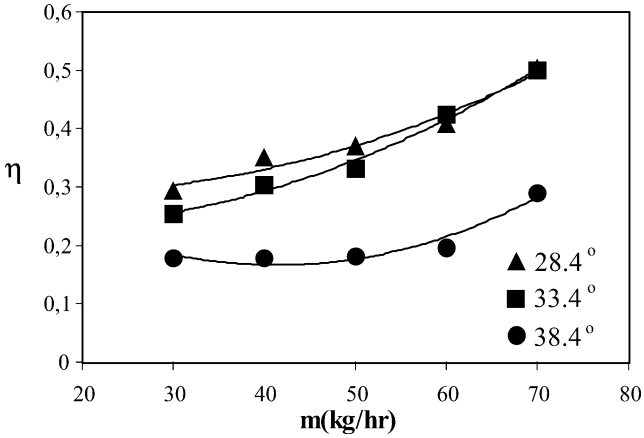

Fig. 10. The changes in instantaneous efficiencies with air flow rates.

4.2. Heat transfer inside the absorber tube

As the flow pattern of the air inside the absorber is turbulent, it may be assumed that the temperature at any measurement point represents the air in the respective cross section or so-called mixing-cup temperature. Daily average values of these temperatures and Eqs. (9) and (11) were used to evaluate local heat transfer coefficients and Colburn factors. Known heat flux, local heat transfer coefficients and local air temperatures were used to find absorber wall temperatures according to $q_x = h(T_w - T_f)$. The results of these computations are given in Table 6.

Film heat transfer coefficients h between air and inner surface of the absorber tube and related Colburn J_H factors computed for various mass flow rates of the air are given in Fig. 11. They can reach up to 25 W·m^{-2}·K^{-1} at 70 kg·h^{-1} air mass flow rate. The film heat transfer coefficients in the industrial air heating and cooling may be up to 50 W·m^{-2}·K^{-1} depending on the systems. But, they are generally low in the operations utilizing solar air heating systems and are reported as below 15 W·m^{-2}·K^{-1} [33]. The relation between Re numbers and heat transfer coefficients h and Colburn J_H factors can be expressed best by power models as following.

$$h = 0.0123(Re)^{0.7626} \quad (r = 0.9997) \tag{13}$$

$$J_H = 0.0136(Re)^{-0.154} \quad (r = 0.9890) \tag{14}$$

4.3. Economical analysis of the system

Economical analysis was carried out for 8 working hours during whole year to compare the annual total cost of the

Table 6
Mean film and absorber temperatures, film heat transfer coefficients and Colburn factors at all the tilting angles and flow rates of the air

m	Thermocouple	$\theta = 28°.4'$				$\theta = 33°.4'$				$\theta = 38°.4'$			
(kg·hr^{-1})	location	T_f	T_p	h	J_H	T_f	T_p	h	J_H	T_f	T_p	h	J_H
70	1	31.50	35.34	25.45	0.00298	36.65	48.04	25.19	0.00295	36.74	46.06	25.18	0.00295
	2	37.90	72.35	25.12	0.00294	41.10	65.20	24.99	0.00292	39.33	53.33	25.06	0.00293
	3	45.10	84.48	24.75	0.00289	45.00	66.27	24.82	0.00290	42.00	56.47	24.95	0.00291
	4	51.80	89.02	24.39	0.00284	48.20	65.75	24.69	0.00288	45.11	62.08	24.82	0.00290
	5	58.12	93.73	24.05	0.00280	51.24	68.03	24.55	0.00286	48.99	70.34	24.65	0.00287
60	1	32.71	41.34	22.45	0.00307	37.78	53.66	22.21	0.00303	37.77	46.56	22.21	0.00303
	2	40.60	81.98	22.11	0.00302	42.80	69.24	22.03	0.00300	40.80	56.70	22.10	0.00302
	3	48.80	92.47	21.80	0.00297	47.00	69.29	21.87	0.00298	44.16	61.88	21.97	0.00300
	4	55.50	91.65	21.54	0.00293	50.93	71.95	21.72	0.00296	47.85	67.49	21.83	0.00297
	5	59.69	82.52	21.37	0.00290	54.39	73.00	21.58	0.00293	51.10	68.47	21.71	0.00295
50	1	33.70	45.94	19.35	0.00317	38.20	55.53	19.17	0.00314	38.76	50.85	19.15	0.00314
	2	43.40	92.75	19.00	0.00311	43.64	71.31	18.99	0.00311	42.10	59.04	19.04	0.00312
	3	52.20	97.72	18.71	0.00305	49.50	79.67	18.80	0.00307	45.50	62.87	18.93	0.00309
	4	58.70	92.76	18.49	0.00301	53.00	71.13	18.68	0.00305	49.57	70.51	18.80	0.00307
	5	61.92	78.88	18.38	0.00299	56.60	75.38	18.56	0.00302	53.55	74.18	18.66	0.00304
40	1	35.64	46.34	16.12	0.00330	36.61	52.19	16.08	0.00329	40.00	52.75	15.99	0.00327
	2	45.42	93.15	15.84	0.00323	44.88	85.28	15.85	0.00324	42.88	56.90	15.91	0.00325
	3	55.30	104.50	15.56	0.00317	53.26	94.80	15.62	0.00318	47.70	71.32	15.78	0.00322
	4	62.04	96.06	15.37	0.00312	56.63	73.44	15.53	0.00316	52.00	73.27	15.66	0.00319
	5	64.45	76.64	15.30	0.00311	60.75	81.46	15.41	0.00313	55.26	71.50	15.56	0.00317
30	1	40.46	54.49	12.69	0.00346	39.84	57.02	12.70	0.00347	41.60	55.92	12.66	0.00346
	2	52.57	109.20	12.43	0.00338	49.39	93.77	12.50	0.00340	45.30	62.36	12.58	0.00343
	3	61.60	104.55	12.22	0.00332	57.82	97.61	12.31	0.00334	50.40	74.14	12.47	0.00340
	4	66.61	90.70	12.10	0.00328	61.44	78.66	12.22	0.00332	54.90	76.03	12.37	0.00336
	5	69.96	86.17	12.03	0.00326	65.01	82.14	12.14	0.00329	57.62	70.47	12.31	0.00335

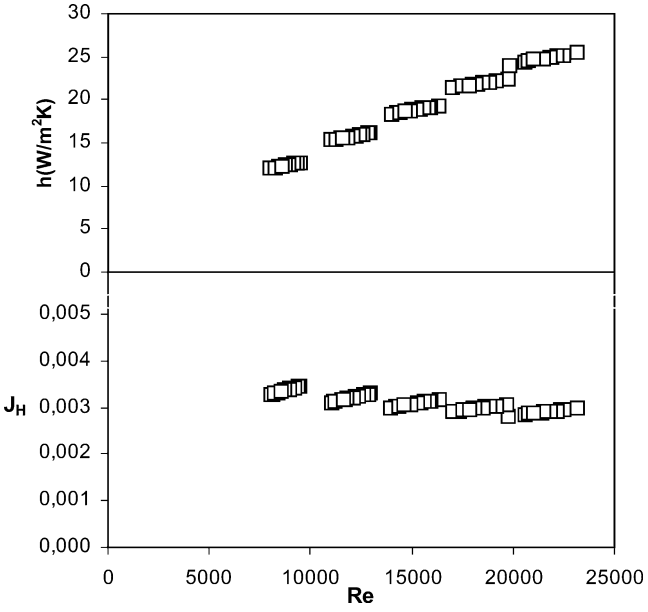

Fig. 11. The correlation between *Re* and/or h and J_H.

present solar air heater with the conventional solar air heater and a conventional electrical heater.

Assuming a depreciation period of 15 years [34], the annual capital cost (ACC) is estimated according to the following equation given by Mitchell [35]:

$$ACC = I(1+j)^n / t_{\text{dep}} \tag{15}$$

Where j, n and I are the annual interest rate taken as 10%, allowed years for loan ($n = 5$ years) and the capital cost respectively and t_{dep} is the number of depreciation years.

The operation cost (energy + maintenance) is evaluated using an electricity rate of US\$ 0.09·kWh^{-1} and annual maintenance cost of 2 to 5% of the capital cost [36].

The annual total cost of the present system is compared with various systems listed in Table 7. These systems have a capital cost of 50 US\$·m^{-2} [37].

When the first investment cost and the annual total cost are considered, the present collector seems more economical than the other systems. But, among the others, the cost of 1 kWh heating is the lowest in the case of the conventional air heater. As the absorbing surface (70 m^2) of the conventional air heater is much more higher than the present collector (0.295 m^2), more useful energy is transferred annually into the air (Q_u), which reduce heating cost.

Investment and operation cost of present solar air heater with conical concentrator and sun tracking mechanism are in acceptable limits as is seen in Table 7. When it's cost and ability to supply air at higher temperatures than those supplied by conventional solar air heaters, it may be preferable in places where hot air is required. By incorporating packing inside the flow channel of the air,

Table 7
Comparison of the annual total cost in US$ for different systems

Item	Systems		
	Conical air heater	Solar air collector*	Conventional electric heater*
Capital cost	480	3500	300
Annual capital cost	51.54	375.79	20.00
Annual maintenance	9.6	70.00	–
Annual energy cost	15.768	82.50	2628.0
Annual total cost	76.91	528.29	2628.0
Cost of 1 kWh heating	0.0427	0.018	0.091

* Values were taken from Abou-Ziyan et al. [37].

more enhancements in the efficiency of the system may be realized. This could make the present collector economically comparable with the conventional solar air heaters.

5. Conclusions

The following results may be drawn from the present work in which forced-convection efficiencies and principal air flow and heat transfer parameters of the solar air heater with conical concentrator have been studied.

Among the tilting angles tested, the lowest 28.4° is the most efficient angle leading up to 50% efficiencies and 82 °C air outlet temperatures at the minimum flow rate (30 $kg{\cdot}h^{-1}$) and the maximum increase (37.2 °C) in the temperature of the air.

The efficiency values acquired by the present conical solar collector are close, but outlet temperatures are approximately twice those reported for conventional flat-plate solar collectors without any packing in the passage space of the air.

Film heat transfer coefficient between air and inner surface of the absorber can reach up to 25 $W{\cdot}m^{-2}{\cdot}K^{-1}$ at 70 $kg{\cdot}h^{-1}$ air mass flow rate.

Further work is needed to elucidate the influence on the efficiencies of some other parameters such as incorporating packing materials into the air passage and using selective absorption surfaces.

Acknowledgement

This study was supporte by the Research Foundation of Fırat University (Project No: FÜNAF-296).

References

[1] K.S. Ong, Thermal performance of solar air heaters-experimental correlation, Solar Energy 55 (3) (1995) 209–220.
[2] R. Verma, R. Chandra, H.P. Garg, Optimization of solar air heaters of different designs, Renewable Energy 2 (4/5) (1992) 521–531.
[3] A.K. Bhargava, H.P. Garg, V.K. Sharma, Evaluation of the performance of air heaters of conventional designs, Solar Energy 29 (6) (1982) 523–526.
[4] B.F. Parker, M.R. Lindley, D.G. Colliver, W.E. Murphy, Thermal performance of three solar air heaters, Solar Energy 51 (6) (1993) 467–479.
[5] K.G. Hollands, E.C. Shewen, Optimization of flow passage geometry for air heating, plate type solar collectors, ASME J. Solar Energy Engrg. 103 (1989) 323–330.
[6] M.R. Diab, J.T. Pearson, Heat transfer characteristics of solar air heater incorporating a finned absorber, in: 4th Internat. Conf. Mechanical Power Engineering, 1982, Paper no. III-14, Cairo.
[7] US, Department of Energy (Solar Energy), Research on the applications of solar energy to industrial drying or dehydration processes, in: J.L. Butler (Ed.), Solar Crop Drying Conference Proceedings, 1977, pp. 69–79.
[8] H.E.S. Fath, Thermal performance of a simple design solar air heater with built-in thermal energy storage system, Renewable Energy 6 (8) (1995) 1033–1039.
[9] N.K. Bansal, R. Uhlemann, A. Boettcher, Plastic solar air heaters of novel design, Report Internat. Buroder KFA-Julich Gmbh, Germany, April 1982.
[10] N.K. Bansal, D. Singh, Analysis of a cylindrical plate matrix solar air heater, Solar and Wind Technology 2 (2) (1985) 95–100.
[11] M.N. Metwally, H.A. Heikal, Optimization of plastic bag solar air collectors (PBSAC) for drying of agricultural products, in: Engrg. Res. Bull. of Univ. of Helwan (ERBUH), Cairo, Vol. 2, 1987.
[12] C. Choudhury, H.P. Garg, Evaluation of a jet plate solar air heater, Solar Energy 46 (4) (1991) 199–209.
[13] P.D. Smith, Solar collector with conical element, US Patent, 1977.
[14] M. Uroshevich, Solar collector, US Patent, 1981.
[15] B.L. Mc Lean, Solar collector device, US Patent, 1989.
[16] P.E. Mather, S.T. Sherlock, Solar energy collector tube, US Patent, 1979.
[17] W.H. Sims, Evacuated envelope and solar energy receiver, US Patent, 1982.
[18] M.J. O'Neill, Solar collector and energy collection system, US Patent, 1978.
[19] R. Winston, Cylindrical radiant energy direction device with refractive medium, US Patent, 1978.
[20] ASHRAE Standard, Methods of Testing to Determine the Thermal Performance of Solar Collectors, American Society of Heating, Refrigerating, and Air-Conditioning Engineers, New York, 1978, pp. 93–77.
[21] H.C. Hottel, A. Whillier, Evaluation of flat-plate solar collector performance, Pub. No. 53, Solar Energy Conversion Research Project, Mass. Inst. of Technology, 1955.
[22] R.W. Bliss, The derivations of several 'plate-efficiency factors' useful in the design of flat-plate solar heat collectors, Solar Energy 3 (4) (1959) 55–64.
[23] J.A. Duffie, W.A. Beckman, Solar Engineering of Thermal Processes, 2nd Edition, Wiley, New York, 1991.
[24] B.N. Prasad, J.S. Saini, Effect of artificial roughness on heat transfer and friction factor in solar air heater, Solar Energy 41 (1988) 555–560.
[25] ASHRAE, Handbook of Fundamentals, American Society of Heating, Refrigerating and Air-Conditioning Engineers, Atlanta, 1989.

[26] G.O.G. Löf, D.A. Fester, J.A. Duffie, Energy balance on a parabolic cylinder solar reflector, ASME J. Engrg. Power A 84 (1962) 24.

[27] I.T. Toğrul, The use of a solar energy system with conical concentrator in drying, Ph.D. Thesis, Dept. of Chemical Engineering, Fırat University, Elazığ, Turkey, 2001.

[28] Methods of testing to determine the thermal performance of solar collectors, ASHRAE Standard 93-77, 1977.

[29] M.L. Khanna, Design data for solar heating of air using a heat exchange and storage system, Solar Energy 11 (1967) 3–4.

[30] N.K. Bansal, R. Uhleman, Development and testing of low cost solar energy collectors for heating air, Solar Energy 33 (2) (1984) 197–208.

[31] M.N. Metwally, H.Z. Abou-Ziyan, A.M. El-Leathy, Performance of advanced corrugated-duct solar air collector compared with five conventional designs, Renewable Energy 10 (4) (1997) 519–537.

[32] S. Satcunanathan, S. Deonarine, A two-pass solar air heater, Solar Energy 15 (1973) 41–49.

[33] O.S.C. Headley, W. Hinds, Medium scale solar crop dryers for agricultural products, in: G. Grossman (Ed.), Proceedings of the International solar energy Society Solar World Congress, Jerusalem, Israel, Vol. III, 1999, pp. 175–179.

[34] W.P. Jones, Air-conditioning Applications and Designs, Arnold, London, 1980.

[35] J.W. Mitchell, Energy Engineering, Wiley, New York, 1983.

[36] P.C. Koelet, T.B. Gray, Industrial Refrigeration: Principal, Design and Applications, Dekker, New York, 1992.

[37] H.Z. Abou-Ziyan, M.F. Ahmed, M.N. Metwally, H.M. Abd El-Hameed, Solar-assisted R22 and R134a heat pump systems for low-temperature applications, Appl. Thermal Engrg. 17 (5) (1977) 455–469.